DOI: 10.1002/chem.201101045

Click-Dendronized Poly(amide–triazole)s—Effect of Dendron Size and Polymer Backbone Symmetry on Self-Assembling and Gelation Properties

Hak-Fun Chow,*[a, b, c, d] Kwun-Ngai Lau,[a] and Man-Chor Chan[a]

Abstract: Nine dendronized poly(amide–triazole)s **2-G*m*G*n*** ($m=1$–3, $n=1$–3), were prepared by the 1:1 copolymerization between AA-type dendritic diazides **4-G*m*** ($m=1$–3) and BB-type dendritic diacetylenes **5-G*n*** ($n=1$–3) under the copper(I)-mediated click coupling conditions. The degree of polymerization value of the polymers was found to range from 15–50, and decreased with increasing size of the dendron, suggesting steric hindrance had a retardation role on the copolymerization efficiency. Based on FT-IR and ^{1}H NMR studies, it was found that significantly strong, interchain hydrogen bonding between the amide units was present in the solution state after copolymerization, whereas the monomers **4-G*m*** and **5-G*n*** were devoid of any intermolecular hydrogen-bonding interaction. Hence a positive allosteric hydrogen-bonding effect was observed after polymerization, and could be rationalized by the zip effect. The strength of the interchain association in polymers **2-G*m*G*n*** was found to decrease with increasing size of the dendron (i.e., **2-G1G1** > **2-G1G2** > **2-G2G1** ≈ **2-G2G2** > **2-G1G3** ≈ **2-G3G1** > **2-G2G3** ≈ **2-G3G2** > **2-G3G3**). Among the nine polymers, only **2-G1G2** and **2-G2G1** were good organogelators for aromatic solvents, while the **2-G2G2** polymer, bearing the closest structural resemblance to the previously reported organogelator **1-G2** prepared from the polymerization of AB-type monomers, was devoid of gelating power. Careful analysis of structures of the present polymer series **2-G*m*G*n*** and the previously reported series **1-G*n*** suggested that the polymer backbone symmetry played a subtle role in controlling their self-assembling and gelating properties.

Keywords: click chemistry • dendrimers • gels • self-assembly

Introduction

The copper(I)-catalyzed cycloaddition (CuAAC) reaction[1] between acetylenes and azides has become an important synthetic tool in many research disciplines and in polymer chemistry.[2,3] While it is a useful and universal ligation technique that can link various types of molecules together, the product functionality, that is, the triazole unit, and its associated properties generated from this reaction have also been the subject of increasing interest. In particular, emerging examples indicate that oligo- and poly(triazole) compounds exhibit some interesting conformational and supramolecular properties.[4] For example, oligotriazoles have been reported as hosts for anions,[5] and to form double helical structures when replacing the phosphodiester linkages in an DNA oligomer.[6] Poly(triazole)s are also known to function as hydro-[7] as well as organogelators.[8] We earlier reported the interesting self-assembling properties of a series of click-dendronized poly(amide–triazole)s **1-G*m*** ($m=1$–3) prepared from the polymerization of AB-type monomers **3-G*m***, in which a synergistic cooperative hydrogen-bonding effect and dendrimer-generation-specific organogelating properties were found.[9,10] Despite these findings, the mechanism by which triazole and the dendritic units, as well as the polymer backbone, exert their control on the supramolecular properties still deserve further investigations. Herein, we disclose additional research findings based on the study of a new series of click-dendronized poly(amide–triazole)s **2-G*m*G*n*** ($m=1$–3; $n=1$–3) bearing alternating dendritic side chains of different size, and provided additional insights of the structural factors on their organogelating and self-assembling properties. These new dendronized polymers were synthesized by a copolymerization reaction between AA-type diazide **4-G*m*** and BB-type diacetylene **5-G*n*** monomers. In contrast to our earlier report in which only three dendronized polymers were subjected to our investigation, here a total number of nine dendronized copolymers of different dendritic side-chain combination were probed in a systematic manner, and hence a broader picture

---

[a] Prof. Dr. H.-F. Chow, Dr. K.-N. Lau, Prof. Dr. M.-C. Chan
Department of Chemistry
The Chinese University of Hong Kong
Shatin NT (Hong Kong)
Fax: (+852) 26035057
E-mail: hfchow@cuhk.edu.hk

[b] Prof. Dr. H.-F. Chow
The Center of Novel Functional Molecules
The Chinese University of Hong Kong
Shatin NT (Hong Kong)

[c] Prof. Dr. H.-F. Chow
Institute of Molecular Functional Materials
Areas of Excellent Scheme
University Grants Committee (Hong Kong)

[d] Prof. Dr. H.-F. Chow
State Key Laboratory on Synthetic Chemistry (Hong Kong)

Supporting information for this article is available on the WWW under http://dx.doi.org/10.1002/chem.201101045.

of the structure–property relationships is revealed. Despite their structural similarities, there are subtle differences between these two series of dendronized polymers **1-G*m*** and **2-G*m*G*n***. In our previous reported polymers **1-G*m***, the unsymmetrical repeating units of the polymer backbone are connected in a head-to-tail manner, and hence the corresponding dipoles are aligned in a parallel fashion (Scheme 1). On the other hand, the same backbone repeating units are arranged either in a head-to-head or tail-to-tail arrangement in **2-G*m*G*n***. As a result, any two neighboring backbone dipoles are aligned in an antiparallel manner. Surprisingly, while only **1-G2** showed gelation properties in our previous study, its closest structural analogue **2-G2G2** in this present series is non-gelating. Hence the results obtained here suggest that the parallel and antiparallel arrangements of these backbone dipoles can also exert substantial influence on the polymer gelaton properties.

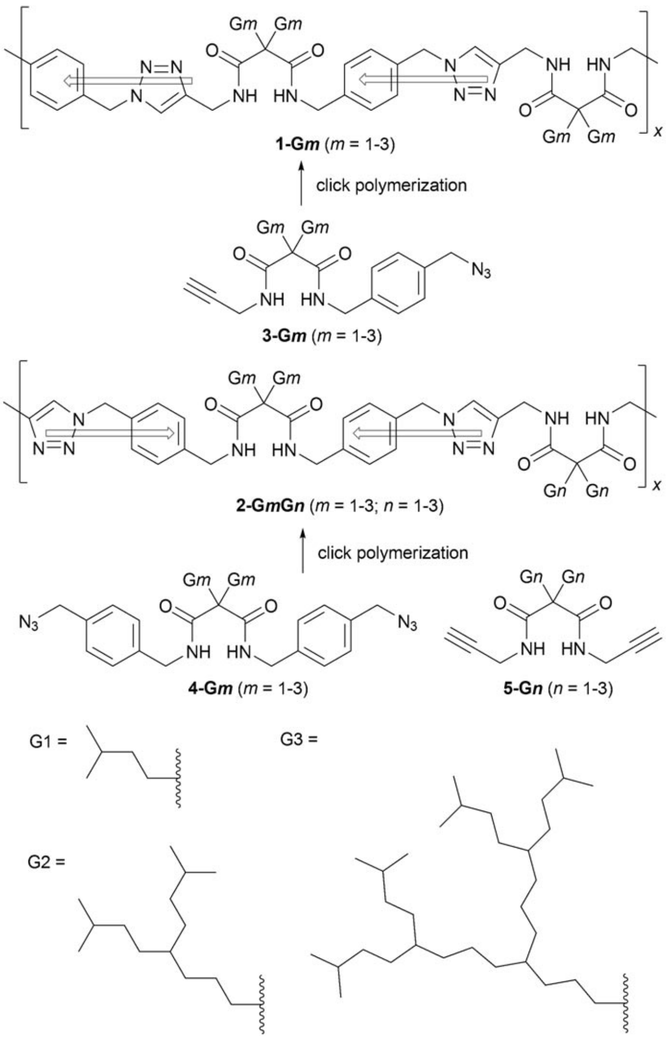

Scheme 1. Click dendronized poly(amide–triazole)s **1-G*m*** from polymerization of AB-type monomers **3-G*m***, and **2-G*m*G*n*** from copolymerization of AA-type **4-G*m*** + BB-type **5-G*n*** monomers.

Results and Discussion

Synthesis: The dendronized copolymers **2-G*m*G*n*** were prepared by the AABB-type click copolymerizations between diazides **4-G*m*** ($m=1$–3) and diacetylene dendritic macromonomers **5-G*n*** ($n=1$–3; Scheme 2). Despite their structural simplicities, direct bis-functionalization of the known dicarboxylic acid dendrons **6-G*m*** ($m=1$–3)[11] with propargyl amine or 4-(azidomethyl)benzyl amine using dicyclohexylcarbodiimide (DCC) or 1-[3-(dimethylamino)propyl]-3-ethylcarbodiimide methiodide (EDCI) failed to give any products. Reactions using the corresponding diacid chlorides, however, led to a complex mixture of products. Hence, sequential introduction of the azide or acetylene functionalities was used. The known monoacid monoesters **7-G*m***[9] were first coupled to propargyl amine in the presence of 1-hydroxybenzotriazole (HOBt) and a coupling reagent to produce the propargyl amides **8-G*m*** in 80–92 % yield. It was found that EDCI was useful for preparation of the first-generation (G1) dendrimer. On the other hand, DCC plus a catalytic amount of *N*,*N*-dimethylaminopyridine (DMAP) were better suited for the second- and thrid-generation (G2 and G3, respectively) dendrimers. The ester functionality in compounds **8-G*m*** was then hydrolyzed under basic conditions to give the corresponding carboxylic acids **9-G*m*** in 77–92 % yield. Finally, coupling of the acids with propargyl amine again under the same coupling conditions afforded the target diacetylenes **5-G*m*** in 80–94 % yield. The target diazides **4-G*m*** were similarly prepared in 67–79 % by reacting the known acids **10-G*m***[9] with 4-(azidomethyl)benzyl amine under the standard coupling conditions. The struc-

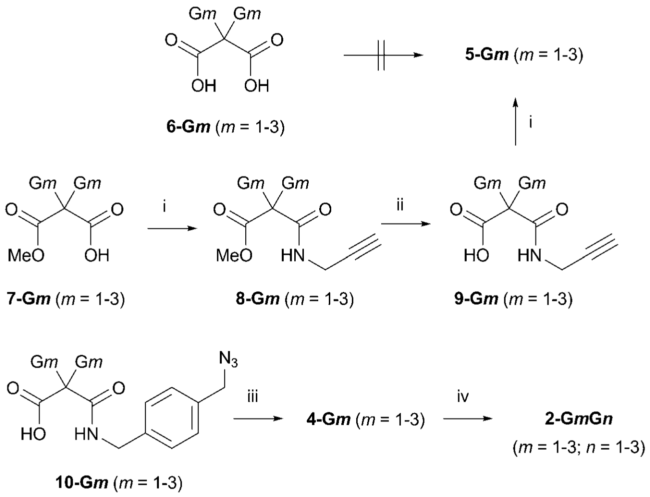

Scheme 2. Synthesis of bifunctional monomers **4-G*m*** and **5-G*m*** and dendronized periodic polymers **2-G*m*G*n***. Reagents and conditions: i) $HC\equiv CCH_2NH_2$, EDCI (or DCC, cat. DMAP), HOBt, CH_2Cl_2; ii) KOH (2 M), THF, MeOH; iii) 4-(azidomethyl)benzylamine, EDCI (or DCC and cat. DMAP), HOBt, CH_2Cl_2; iv) **5-G*n*** (1 equiv), $CuSO_4\cdot 5H_2O$, sodium ascorbate, $THF/DMF/H_2O$ (v/v/v 1:1:1).

tures of all compounds were fully characterized and confirmed by ^{1}H and ^{13}C NMR spectroscopy and mass spectrometry. Their purities were also assessed by size exclusion chromatography (SEC), and all of them gave a major sigmodial peak with a polydispersity index (PDI) of less than 1.03 (see Supporting Information for details).

Click copolymerizations: The procedure for the 1:1 click polymerizations between **4-G*m*** and **5-G*n*** was the same as that described for the preparation of dendronized polymers **1-G*m***.[9] To ensure good polymerization efficiency, a 1:1:1 mixture of THF, DMF, and water was required to maintain homogeneous conditions, at least in the initial stage of the polymerization. After stirring at 25 °C for four days, the polymer was isolated either by precipitation in aqueous HCl, or by extraction with CH_2Cl_2 followed by solvent evaporation. A total of nine dendronized polymers was prepared in yields from 84–99 %. It should be noted that dendronized polymer **2-G*m*G*n*** was structurally different from **2-G*n*G*m***.

The structure of the various dendronized polymers was first characterized by ^{1}H NMR spectroscopy. To minimize the degree of aggregations, [D$_8$]THF was employed as the solvent for analysis except for **2-G1G1**, which was only soluble in [D$_6$]DMSO. Both the acetylene and methylene proton signals adjacent to the azide functionality disappeared, and hence this suggested that the copolymerization reactions were very efficient. The ^{1}H signals of the aliphatic hydrocarbon dendrons remained almost unchanged, but a certain degree of peak broadening was observed. Two methylene ^{1}H signals (ArCH_2Triaz and ArCH_2N) appeared at $\delta = 4.2$–4.5 ppm, whereas the third (NCH_2Triaz) was located at $\delta = 5.2$–5.7 ppm. All three methylene ^{1}H signals were shifted downfield relative to their corresponding ^{1}H signals in the monomers. The aromatic signals of all dendronized polymers appeared at around $\delta = 7.0$–7.3 ppm either as a broad singlet or multiplets, while the ^{1}H signal of the triazole ring was situated at about $\delta = 7.4$–7.8 ppm.

The position of the N–H signals of this new series of dendronized polymers deserved further comments. As **2-G1G1** is only soluble in DMSO, the N–H signals appeared at a relatively downfield region at about $\delta = 8.5$–9.0 ppm (see Supporting Information for details). For the remaining eight soluble dendronized polymers, at least three sets of amide ^{1}H signals at about $\delta = 7.4$–8.5 ppm could be identified (Figure 1). This was in sharp contrast to the spectral properties of the previously reported **1-G2**, which was found to be a good organogelator in THF, wherein the NH signals were significantly shifted downfield to $\delta = 10.5$–10.7 ppm. As it turned out, none of the nine new dendronized polymers, including the closest structural isomer of **1-G2** (i.e., **2-G2G2**), were able to gel THF, highlighting that a subtle change of polymer backbone could significantly alter their self-assembling and organogelating properties.

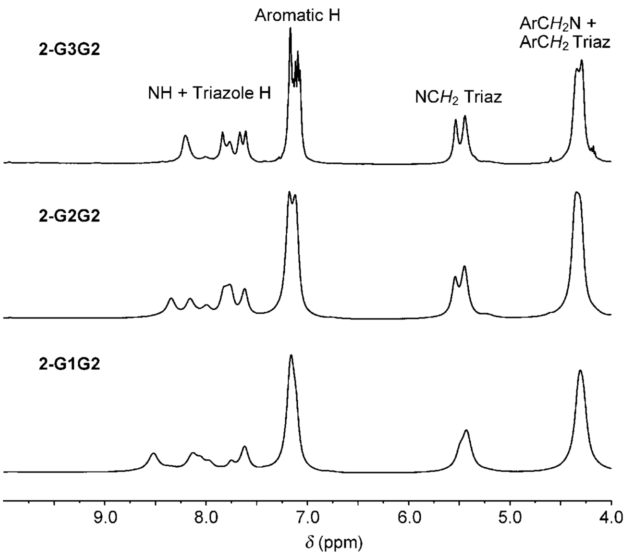

Figure 1. Stacked partial ^{1}H NMR (400 MHz, [D$_8$]THF, 25 °C) spectra of dendronized polymers **2-G*m*G2**. For clarity, the spectral portion due to the aliphatic hydrocarbon dendron was not shown.

The ^{13}C NMR signals of all nine dendronized polymers **2-G*m*G*n*** were well resolved. Hence, two sp^{2}-hybridized ^{13}C signals due to the triazole appeared as two distinctive peaks at about $\delta = 123.0$ and 147.0 ppm. The ^{13}C signals due to the carbonyl moiety were located at about $\delta = 172.5$–174.0 ppm. In the cases of **2-G1G1** and **2-G2G1** dendronized polymers, only one ^{13}C carbonyl signal was found, but up to five signals were noted in the case of **2-G3G3** (Figure 2). Hence, one could conclude that dendronized polymers constructed from monomers bearing G1 dendrons showed a high structural homogeneity with respect to those from monomers of G2 and G3 dendrons, indicating that the steric bulkiness of the dendritic appendage lowered the copolymerization efficiency. This finding is also consistent with the results obtained from size exclusion chromatographic (SEC) analysis (vide infra).

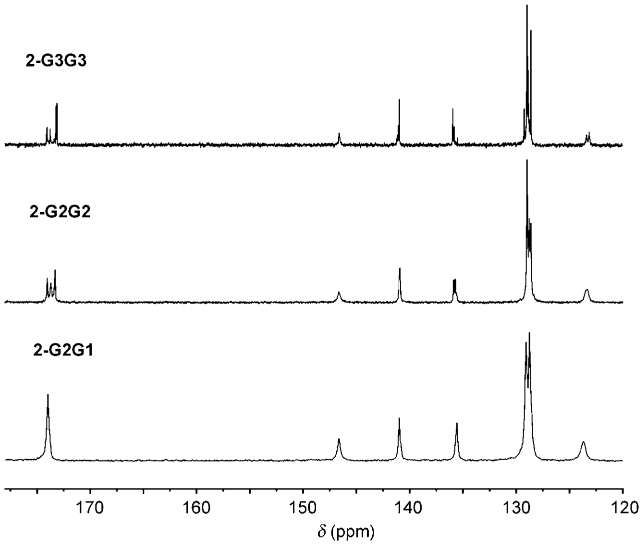

Figure 2. Stacked partial ^{13}C NMR (100 MHz, [D$_8$]THF, 25 °C) spectra of dendronized polymers **2-G3G3**, **2-G2G2** and **2-G2G1**. Only the C=O, aromatic and triazole ^{13}C signals were shown.

The dendronized polymers **2-G*m*G*n*** were then characterized by SEC analysis. Similar to **1-G1**, the poor solubility properties of **2-G1G1** in THF precluded its SEC examination. In addition to the expected polymer peak, the SEC chromatograms of all examined dendronized polymers also showed the presence of many low-molecular-weight (LMW) peaks, suggesting the formation of cyclic oligomers during the copolymerization process[9] (see Supporting Information for details). The calculated M_w, PDI, degree of polymerization (DP) values, and weight percentage of LMW oligomers (up to [3+3]mer) are given in Table 1. One point that should be mentioned here was that the DP values were calculated based on the molecular weight of one repeating unit. For **2-G*m*G*n***, one repeating unit actually consists of two dendron anchorage points, and thus the DP values should be doubled if we want to directly compare them with the results obtained from **1-G*m***. Taking this into consideration, it was noted that there was little difference in terms of the PDI and DP values, and also in the weight% of LMW fraction between polymers **1-G*m*** and **2-G*m*G*n*** bearing dendritic appendages of the same generation.

Table 1. SEC data of dendronized polymers **2-G*m*G*n***.[a]

	M_w	PDI	DP	Weight% of LMW fraction[b]
2-G1G1[c]	–	–	–	–
2-G1G2	56000	2.3	51	1
2-G1G3	33000	1.6	21	5
2-G2G1	43000	1.9	39	2
2-G2G2	39000	2.1	29	4
2-G2G3	27000	1.5	15	8
2-G3G1	41000	1.7	26	5
2-G3G2	46000	2.0	25	5
2-G3G3	45000	1.9	19	8

[a] All experiments were conducted in THF at 40°C using polystyrenes as calibration standards. [b] Low MW fraction up to [3+3]mer. [c] Not determined because of poor solubility in THF.

Gelation properties: In the present study, nine compounds were synthesized with a broader structural spectrum in order to have a better understanding of the size of the dendrons on the self-assembling and gelation properties. Recall that in our previous series of dendronized polymers **1-G*m***, three compounds were prepared and only the G2-dendronized polymer **1-G2** could form gels with organic solvents. To our surprise, its closest structural analogue **2-G2G2** could not form gels with any organic solvents. Among the nine compounds, only **2-G1G2** and **2-G2G1** were good organogelators. Other dendronized polymers just simply dissolved in most organic solvents, while **2-G1G1** was not soluble in most nonpolar organic solvents.

The gelation properties of **2-G1G2** and **2-G2G1** were further examined in various solvents (Table 2). One point that should be mentioned was that experiments were conducted on polymer samples after treatment with ethylenediaminetetraacetic acid (EDTA) to remove trace of the Cu ions. In contrast to dendronized polymer **1-G2**, polymers **2-G1G2** and **2-G2G1** formed organogels specifically with aromatic solvents, but did not form gel in other non-aromatic organic solvents. In addition, the gelation speed of organogels originated from polymers **2-G1G2** (≈20 min) and **2-G2G1** (≈1 h) were slower than that from **1-G2** (≈5 min). Moreover, the minimum gelation concentrations (MGC) for both of them were higher than those of polymer **1-G2**, and hence one could conclude that the presence series of dendronized polymers **2-G1G2** and **2-G2G1** had a lower gelation power.

Table 2. MGC values [mg mL^{-1}] of **2-G1G2** and **2-G2G1** dendronized polymers in various organic solvents.[a]

Solvent	2-G1G2	2-G2G1	Solvent	2-G1G2	2-G2G1
n-hexane	– (I)	– (I)	toluene	20 (CG)	30 (CG)
$CHCl_3$	– (S)	– (S)	*o*-xylene	10 (CG)	50 (CG)
EtOAc	50 (OG)	– (S)	*m*-xylene	20 (CG)	50 (CG)
acetone	– (S)	– (S)	*p*-xylene	20 (CG)	30 (CG)
EtOH	– (S)	– (S)	*o*-dichlorobenzene	10 (CG)	20 (CG)
THF	– (S)	– (S)	anisole	20 (CG)	50 (CG)
benzene	50 (CG)	20 (CG)	nitrobenzene	50 (TG)	– (S)

[a] CG = transparent gel; OG = opaque gel; TG = translucent gel; S = soluble (> 50 mg mL^{-1}); I = insoluble.

The thermotropic behavior of the gels from polymers **1-G2**, **2-G1G2**, and **2-G2G1** in *p*-xylene were studied by using the dropping ball method. For the gel derived from dendronized polymer **2-G2G1**, the steel ball sank immediately to the bottom of the vial when it was placed on the gel surface before heating. This indicated that polymer **2-G2G1** was the weakest organogelator among the three. For dendronized polymer **2-G1G2**, as a 8% (w/v) gel, the T_g was near to the boiling point of *p*-xylene (136°C). However, when the concentration was reduced to 7% (w/v), the T_g decreased significantly (124°C). A T_g temperature plateau at 124°C was observed from 7% (w/v) to 2.5% (w/v), followed by an abrupt drop to 72°C as the concentration was lowered to 2% (w/v). On the other hand, the gel derived from polymer **1-G2** showed significantly higher T_g (130°C) than polymer **2-G1G2** even at a lower concentration range (1.5–3% w/v). This again showed that **2-G1G2** was a weaker organogelator than **1-G2**, even though the former possessed a higher DP and a larger M_w value.

Gelation mechanism: To unveil the mechanism of the self-assembling process, FT-IR spectroscopy was used to probe the extent of hydrogen bonding in all dendronized monomers **4-G*m*** and **5-G*n*** and the click polymers **2-G*m*G*n*** (Table 3). For both the diazides **4-G*m*** and the diacetylenes **5-G*n***, the C=O stretching frequencies were located at about 1679 and 1682 cm^{-1}, respectively. These values are typical of non-hydrogen-bonded C=O stretching frequency. Furthermore, two N–H absorptions were observed at about 3433 and 3280 cm^{-1} in all generations of monomers. While the one at 3433 cm^{-1} was characteristic of a non-hydrogen-bonded secondary amide, the one at 3280 cm^{-1} appeared to be due to hydrogen-bonded N–H stretching. However, this assignment contradicted other experimental evidence. First,

Table 3. FT-IR data [cm^{-1}] of **4-G*m***, **5-G*n*** monomers and dendronized polymers **2-G*m*G*n*** in different physical states.[a]

	State	N–H	≡C–H	N_3	C=O
4-G1	solution[b]	3433, 3276	–	2099	1679
4-G2	solution[b]	3433, 3279	–	2099	1679
4-G3	solution[b]	3433, 3277	–	2099	1679
5-G1	solution[b]	3434, ≈3290[c]	3306	–	1682
5-G2	solution[b]	3433, ≈3290[c]	3310	–	1682
5-G3	solution[b]	3434, ≈3290[c]	3311	–	1682
2-G1G1	solid	3341	–	–	1663
2-G1G2	dried gel	3334	–	–	1640
	gel[d]	3341	–	–	1643
2-G1G3	solid	3336	–	–	1643
	solution[d]	3341	–	–	1666
2-G2G1	dried gel	3341	–	–	1652
	gel[d]	3337	–	–	1649
2-G2G2	solid	3344	–	–	1643
	solution[d]	3344	–	–	1648
2-G2G3	solid	3337	–	–[e]	1647
	solution[d]	3341	–	–[e]	1673
2-G3G1	solid	3345	–	–[e]	1647
	solution[d]	3342	–	–	1665
2-G3G2	solid	3335	–	–	1643
	solution[d]	3345	–	–	1673
2-G3G3	solution[d]	3346	–	–[e]	1676

[a] Spectra were recorded at 2 cm^{-1} resolution. [b] 35 mM solution in toluene. [c] Exact frequency of the latter number could not be determined due to overlapping with ≡C–H stretching. [d] ≈4 % w/v in toluene. [e] A residual N_3 absorption peak was found at 2099 cm^{-1}.

this was inconsistent with the ^{1}H NMR results, in which the N–H signal appeared at an upfield position ($\delta = 7.4$–7.5 ppm) for all the dendritic monomers, which indicated little or no hydrogen bonding in the solution state. Second, a ^{1}H NMR concentration-dependent study was carried out using diazide **4-G3** in [D$_8$]toluene. No significant shift in N–H signal ($\Delta\delta \leq 0.05$ ppm) was found in concentrations in the range 35–0.78 mM. Third, if N–H hydrogen bonding was present in the monomers, the C=O stretching band should be redshifted. However, all the C=O stretching bands appeared at about 1680 cm^{-1}, a region that corresponded to non-hydrogen-bonded C=O stretching. It should be noted that the IR absorption band at 3280 cm^{-1} could not be found in all the asymmetrical AB-type dendritic monomers **3-G*m*** used in the preparation of **1-G*m***, while this peak was observed in all the symmetrical **4-G*m*** and **5-G*n*** monomers.

Careful examination of the literature suggested that two types of N–H stretching modes were possible for the symmetrical AA-type **4-G*m*** and BB-type **5-G*n*** monomers, namely symmetrical and asymmetrical. Strictly speaking, only those bonds with the same symmetry can be coupled to give this kind of interactions in IR spectroscopy. Taking this into consideration, it could be easily rationalized why the previous AB-type monomers **3-G*m*** did not show this kind of band splitting, as the two N–H bonds did not have the same symmetry. In fact, the N–H stretchings of symmetrical malonamide[12] were found to split into two bands (3375 and 3162 cm^{-1}) in the solid state, attributable to the asymmetric and symmetric N–H stretchings, respectively. It could therefore be concluded that N–H stretching signal at ≈3280 cm^{-1} of the symmetrical **4-G*m*** and **5-G*n*** monomers was due to band splitting and not hydrogen bonding. In other words, all monomers **4-G*m*** and **5-G*n*** are non-hydrogen-bonded in the solution state. This was consistent with what was found with the unsymmetrical monomers **3-G*m***.

For the IR spectra of the dendronized polymers **2-G*m*G*n***, some showed the presence of a residual N_3 absorption peak (e.g., **2-G2G3** and **2-G3G1** in the solid state, **2-G2G3** and **2-G3G3** in the solution state). Hence, this suggested that either the polymerization was not 100 % complete, and/or the degree of polymerization was low. The former situation would lead to the presence of residue diazide and/or diacetylene monomers, while the latter would render the higher percentage of the azide or alkyne end groups detectable by IR spectroscopy. Unfortunately, the residual ≡C–H peak, if any, was obscured by the broader N–H signals and could not be observed. Apparently, ^{1}H NMR spectroscopy was a less sensitive tool to monitor the extent of the polymerization, as no acetylenic proton signals could be observed in all the ^{1}H NMR spectra of the polymers **2-G*m*G*n*** (see above). The presence of the N_3 absorption peaks revealed that the efficiency of the AABB-type copolymerization were inferior to that of the AB-type polymerization involving the unsymmetrical monomers **3-G*m***. Nonetheless, we could not absolutely rule out this was the result due to a weighing error of the monomers, as this type of AABB-type polymerization required an exact 1:1 reactant stoichiometry.

For the solid-state FT-IR spectra, all dendronized polymers gave one broad N–H peak between 3335–3345 cm^{-1} and a C=O peak between 1643–1663 cm^{-1} (see Supporting Information for details). Both signals were redshifted relative to those of the monomers in toluene, and were indicative of the presence of intra- and/or interchain hydrogen bonds between the N–H and C=O moieties. Furthermore, the non-hydrogen-bonded N–H peak (≈3430 cm^{-1}) originally present in the monomers disappeared. These findings were in accord to the observed red shifts of C=O and N–H signals in the solid-state FT-IR spectra of most secondary amides.

The solution FT-IR spectra of the non-gelating dendronized polymers (except **2-G1G1** because of its poor solubility) and the toluene gel FT-IR spectra of the two gelating **2-G1G2** and **2-G2G1** polymers were also measured in ≈4 % toluene solution (see Supporting Information for details). Several interesting findings were noted. First, the N–H signal of all dendronized polymers was redshifted (≈130 cm^{-1}) to about 3341–3346 cm^{-1}, indicating the presence of hydrogen bonding in the solution state. Second, there was the presence of a shoulder peak at around 3430 cm^{-1} in dendronized polymers that contained the larger G2 and G3 dendrons (i.e., **2-G2G3**, **2-G3G2**, **2-G3G3**), but this was not observed in dendronized polymers not bearing the largest G3 dendron such as **2-G2G1** (Figure 3). This indicated that the interpolymer chain hydrogen bonding became weaker once the largest G3 dendron was attached to the polymer backbone. Third, in line with this finding, the extent of the C=O red shift was found to re-

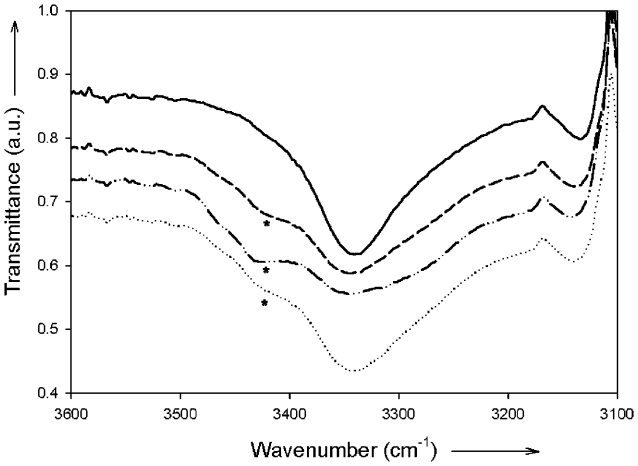

Figure 3. Stacked partial FT-IR spectra of dendronized polymers (from top to bottom) **2-G2G1**, **2-G2G3**, **2-G3G2** and **2-G3G3**. The asterisks (*) indicate the shoulder peak at 3430 cm^{-1}.

flect the increasing degree of hydrogen-bonding interactions with decreasing dendron size (Figure 4). For **2-G2G3**, **2-G3G3**, and **2-G3G2**-dendronized polymers, the position of the C=O signal was between 1673–1676 cm^{-1}, representing a red shift of 5–10 cm^{-1} as compared to that of the non-hydrogen-bonded dendronized monomers (spectral resolution at 2 cm^{-1}). The red shift value was increased to 15 cm^{-1} for **2-G1G3** and **2-G3G1**. For the non-gelating **2-G2G2** and the weaker gelating dendronized polymer **2-G2G1**, a red shift of ≈20 cm^{-1} was found. This shift was further increased to 25 cm^{-1} in the stronger gelating dendronized polymer **2-G1G2**. The freeze-dried gel FT-IR spectra of the two dendronized polymers **2-G1G2** and **2-G2G1** were also recorded. As expected, both the N−H and C=O bands experienced red shift values that were comparable to those observed in the gel state.

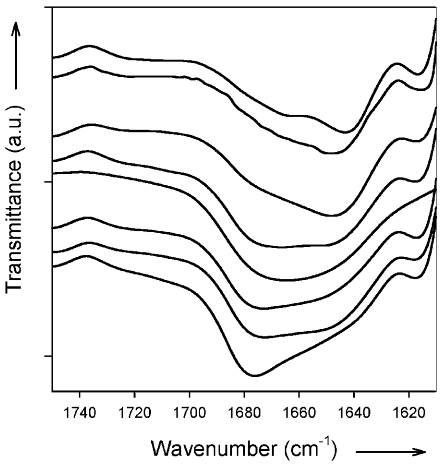

Figure 4. Stacked partial FT-IR spectra of dendronized polymers **2-G*m*G*n***, showing the gradual increase of C=O red-shift with decreasing size of dendritic appendage. From top to bottom: **2-G2G1**, **2-G2G1**, **2-G2G2**, **2-G1G3**, **2-G3G1**, **2-G2G3**, **2-G3G2**, and **2-G3G3**.

In summary, the FT-IR experimental results reinforced our earlier proposed concept of synergistic binding of the amide units upon polymerization. In addition, the effect of increasing dendron size on impeding the self-assembly properties of such amide-containing dendrimers was clearly revealed. In terms of gelation properties, only dendronized polymers (i.e., **2-G1G2** and **2-G2G1**) bearing dendrons of moderate size were good organogelators. However, what still remained perplexing was why gelation was specific to **2-G1G2** and **2-G2G1**, but not to **2-G2G2**. This last dendronized polymer evidently possesses the closest structural resemblance to the uniquely organogelating **1-G2** in the AB-type dendronized polymers.

In our previous work,[9] we proposed that the strength of polymer self-assembly was controlled by 1) the synergistic association originated from the zip-effect after polymerization, and 2) the size of the dendritic appendage. In order to rationalize the gelation property of **2-G1G2** and **2-G2G1** and also the lack of gelation property of **2-G2G2**, we speculated that there was a third factor involved, namely the polymer backbone symmetry. Careful examination of **1-G2** and **2-G2G2** revealed one subtle structural difference between them. Due to its unsymmetrical nature, the polymer backbone segment between the two dendritic anchorage points should possess a net dipole moment (grey arrows in Figure 5). Based on the studies by Schlüter,[13] it is likely that such dendronized polymers, especially those bearing the G2 and G3 dendrons, will adopt a rigid cylindrical structure. Hence, in the AB-type dendronized polymers **1-G*m***, the adjacent dipoles should be aligned more or less along the same direction (i.e., parallel orientation), resulting in a net polymer backbone dipole. On the other hand, in the AABB-type dendronized polymers **2-G*m*G*n***, the adjacent

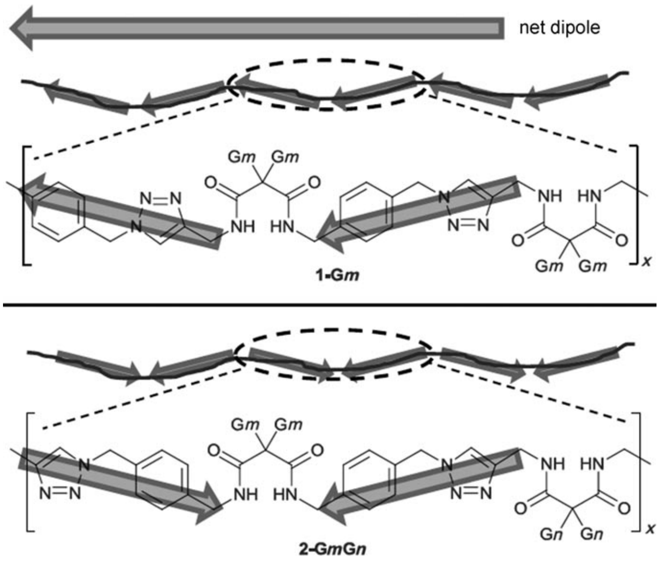

Figure 5. The arrangement of backbone dipoles (shown as arrows) in the AB-type **1-G*m*** and AABB-type **2-G*m*G*n*** dendronized polymers.

dipoles are aligned in antiparallel fashion, and this type of polymer is expected to have a diminishing overall dipole moment due to the cancellation effect of the antiparallel arrangement. Hence, the interchain interaction between the parallel-type polymer chains (i.e., **1-G*n***) should be stronger than that between the antiparallel-type polymer chains (i.e., **2-G*m*G*n***), because of the presence of extra dipole–dipole interaction. Hence, the absence of a dipole–dipole interaction in case of **2-G2G2**, as compared to the presence of dipole–dipole interaction in **1-G2**, weakened the interchain association, making it a poor organogelator. In order to become an effective organogelator, the interchain hydrogen-bonding interaction must be strengthened, and this could be realized by decreasing the size of the appending dendrons. Hence, both **2-G1G2** and **2-G2G1** are good organogelators, as one of the dendrons is smaller and this can promote stronger interchain association and compensate for the diminishing polymer dipole–dipole interaction.

Conclusion

A new series of click poly(amide–triazole) dendronized polymers **2-G*m*G*n*** was prepared by the 1:1 copolymerization of AA-type diazides **4-G*m*** and BB-type diacetylenes **5-G*n***. The DP values of the polymer obtained were comparable to those of the previously reported **1-G*n*** dendronized polymers, and were found to decrease with increasing dendron size. The strength of polymer interchain self-association was found to be influenced by three factors. First, a synergistic hydrogen-bonding interaction, arising due to the presence of many amide units in close proximity and in high spatial regularity along the polymer chain, was identified. Second, the strength of intermolecular self-association was found to decrease with increasing dendron size, indicating that steric repulsion between the polymer side chains also played an important role in defining the binding strength. Third, the polymer backbone symmetry, which can determine the presence or absence of an overall polymer dipole moment, contributes an extra binding factor through the polymer dipole–dipole interaction. Among the nine newly prepared dendronized polymers, only **2-G1G2** and **2-G2G1** were good organogelators for aromatic solvents. In contrast, **2-G2G2**, which possessed the closest structural similarity to the previously reported organogelator **1-G2**, was non-gelating. This differential gelating property could be rationalized in terms of the difference in polymer backbone symmetry.

Experimental Section

G1-Diazide 4-G1: EDCI (0.70 g, 2.36 mmol) was added to a stirred solution of **10-G1** (0.70 g, 1.80 mmol), 4-(azidomethyl)benzylamine (0.38 g, 2.34 mmol), and HOBt (0.32 g, 2.37 mmol) in CH_2Cl_2 (30 mL). The reaction mixture was stirred at 25 °C for 2 h and concentrated under reduced pressure. The residue was purified by flash chromatography on silica gel (eluent: hexane/EtOAc 4:1) to afford **4-G1** (0.76 g, 79%) as a white solid. M.p. 126–128 °C; $R_f=0.16$ (hexane/EtOAc 4:1); ^{1}H NMR (400 MHz, $CDCl_3$): $\delta=0.81$ (d, $J=6.8$ Hz, 12H; CH_3), 1.00–1.12 (m, 4H; CH_2), 1.44 (septet, $J=6.8$ Hz, 2H; C*H*Me$_2$), 1.79–1.91 (m, 4H; CCH_2), 4.32 (s, 4H; CH_2N_3), 4.46 (d, $J=6$ Hz, 4H; NHC*H*$_2$), 7.27 (d, $J=8$ Hz, 4H; Ar*H*), 7.32 (d, $J=8$ Hz, 4H; Ar*H*), 7.51 ppm (t, $J=6$ Hz, 2H; NH); ^{13}C NMR (100 MHz, $CDCl_3$): $\delta=22.3$, 28.1, 33.7, 36.0, 42.9, 54.2, 56.5, 127.8, 128.3, 134.3, 138.5, 173.5 ppm; SEC: $R_t=34.69$ min; MS (ESI): *m*/*z* (%): 555 (100) [*M*+Na$^+$]; HRMS (ESI) calcd for $C_{29}H_{40}N_8O_2+Na^+$: 555.3166; found: 555.3153; elemental analysis calcd (%) for $C_{29}H_{40}N_8O_2$: C 65.39, H 7.57, N 21.03; found: C 65.43, H 7.76, N 21.04.

G2-Diazide 4-G2: DCC (0.72 g, 3.49 mmol) was added to a stirred solution of **10-G2** (1.60 g, 2.50 mmol), 4-(azidomethyl)benzylamine (0.56 g, 3.45 mmol), HOBt (0.47 g, 3.48 mmol), and DMAP (2 mg) in CH_2Cl_2 (30 mL). The reaction mixture was stirred at 25 °C for 2 h and concentrated under reduced pressure. The residue was purified by flash chromatography on silica gel (eluent: hexane/EtOAc 8:1) to afford **4-G2** (1.41 g, 72%) as a white solid. M.p. 74–76 °C; $R_f=0.13$ (hexane/EtOAc 8:1); ^{1}H NMR (400 MHz, $CDCl_3$): $\delta=0.85$ (d, $J=6.8$ Hz, 24H; CH_3), 1.03–1.24 (m, 26H), 1.45 (septet, $J=6.8$ Hz, 4H; C*H*Me$_2$), 1.78–1.88 (m, 4H; CCH_2), 4.32 (s, 4H; CH_2N_3), 4.47 (d, $J=5.6$ Hz, 4H; NHC*H*$_2$), 7.27 (br s, 8H; Ar*H*), 7.49 ppm (t, $J=5.6$ Hz, 2H; NH); ^{13}C NMR (100 MHz, $CDCl_3$): $\delta=22.4$, 22.8, 22.9, 28.5, 31.2, 34.1, 35.9, 37.8, 38.4, 43.4, 54.5, 57.2, 128.1, 128.7, 134.7, 138.5, 173.4 ppm; SEC: $R_t=33.28$ min. MS (ESI): *m*/*z* (%): 808 (100) [*M*+Na$^+$]; HRMS (ESI) calcd for $C_{47}H_{76}N_8O_2+Na^+$: 807.5983; found: 807.5977; elemental analysis calcd (%) for $C_{47}H_{76}N_8O_3$: C 71.90, H 9.76, N 14.26; found: C 71.95, H 10.08, N 14.19.

G3-Diazide 4-G3: DCC (0.61 g, 2.96 mmol) was added to a stirred solution of **10-G3** (1.91 g, 1.67 mmol), 4-(azidomethyl)benzylamine (0.48 g, 2.96 mmol), HOBt (0.37 g, 2.74 mmol), and DMAP (2 mg) in CH_2Cl_2 (30 mL). The reaction mixture was stirred at 25 °C for 2 h and concentrated under reduced pressure. The residue was purified by flash chromatography on silica gel (eluent: hexane/EtOAc 15:1) to afford **4-G3** (1.45 g, 67%) as a pale yellow oil. $R_f=0.25$ (hexane/EtOAc 12:1); ^{1}H NMR (400 MHz, $CDCl_3$): $\delta=0.87$ (d, $J=6.4$ Hz, 48H; CH_3), 1.05–1.30 (m, 70H), 1.48 (septet, $J=6.8$ Hz, 8H; C*H*Me$_2$), 1.78–1.89 (m, 4H; CCH_2), 4.32 (s, 4H; CH_2N_3), 4.47 (d, $J=5.6$ Hz, 4H; NHC*H*$_2$), 7.27 (br s, 8H; Ar*H*), 7.50 ppm (t, $J=5.6$ Hz, 2H; NH); ^{13}C NMR (100 MHz, $CDCl_3$): $\delta=22.4$, 22.87, 22.89, 23.8, 28.5, 31.3, 31.4, 34.0, 34.3, 36.0, 36.1, 37.4, 38.0, 38.4, 43.4, 54.5, 57.2, 128.1, 128.7, 134.7, 138.5, 173.4 ppm; SEC: $R_t=31.72$ min; HRMS (ESI) calcd for $C_{83}H_{148}N_8O_2+Na^+$: 1312.1622; found: 1312.1675; elemental analysis calcd (%) for $C_{83}H_{148}N_8O_2$: C 77.27, H 11.56, N 8.68; found: C 77.34, H 11.90, N 8.69.

G1-Diacetylene 5-G1: EDCI (0.46 g, 1.51 mmol) was added to a stirred solution of **9-G1** (0.32 g, 1.14 mmol), propargylamine (0.16 mL, 2.50 mmol), and HOBt (0.20 g, 1.48 mmol) in CH_2Cl_2 (20 mL). The reaction mixture was stirred at 25 °C for 2 h and concentrated under reduced pressure. The residue was purified by flash chromatography on silica gel (eluent: hexane/EtOAc 3:1) to afford **5-G1** (0.29 g, 80%) as a white solid. M.p. 123.5–126 °C; $R_f=0.39$ (hexane/EtOAc 3:1); ^{1}H NMR (400 MHz, $CDCl_3$): $\delta=0.86$ (d, $J=6.4$ Hz, 12H; CH_3), 1.00–1.20 (m, 4H; CH_2), 1.48 (septet, $J=6.4$ Hz, 2H; C*H*Me$_2$), 1.75–1.95 (m, 4H; CCH_2), 2.22 (t, $J=2.4$ Hz, 2H; $C{\equiv}CH$), 4.06 (dd, $J=5.2$, 2.4 Hz, 4H; $CH_2C{\equiv}C$), 7.40 ppm (br s, 2H; NH); ^{13}C NMR (100 MHz, $CDCl_3$): $\delta=22.5$, 28.2, 29.2, 33.7, 36.3, 56.7, 71.4, 79.5, 173.4 ppm; SEC: $R_t=35.18$ min; MS (ESI): *m*/*z* (%): 341 (100) [*M*+Na$^+$]; HRMS (ESI) calcd for $C_{19}H_{30}N_2O_2+Na^+$: 341.2199; found: 341.2207; elemental analysis calcd (%) for $C_{19}H_{30}N_2O_2$: C 71.66, H 9.49, N 8.79; found: C 71.62, H 9.89, N 8.70.

G2-Diacetylene 5-G2: DCC (0.09 g, 0.44 mmol) was added to a stirred solution of **9-G2** (0.16 g, 0.30 mmol), propargylamine (0.06 mL, 0.94 mmol), HOBt (0.06 g, 0.44 mmol), and DMAP (2 mg) in CH_2Cl_2 (15 mL). The reaction mixture was stirred at 25 °C for 2 h and concentrated under reduced pressure. The residue was purified by flash chromatography on silica gel (eluent: hexane/EtOAc 8:1) to afford **5-G2** (0.16 g, 94%) as a white solid. M.p. 68–69 °C; $R_f=0.42$ (hexane/EtOAc 8:1); ^{1}H NMR (400 MHz, $CDCl_3$): $\delta=0.85$ (d, $J=6.4$ Hz, 24H; CH_3), 1.03–1.26 (m, 26H), 1.44 (septet, $J=6.4$ Hz, 4H; C*H*Me$_2$), 1.74–1.86 (m, 4H; CCH_2), 2.19 (t, $J=2.4$ Hz, 2H; $C{\equiv}CH$), 4.05 (dd, $J=5.2$, 2.4 Hz, 4H;

CH$_2$C≡C), 7.41 ppm (t, J=5.2 Hz, 2H; NH); ^{13}C NMR (100 MHz, CDCl$_3$): δ=22.0, 22.68, 22.72, 28.3, 29.1, 31.0, 33.8, 35.7, 37.5, 38.7, 56.8, 71.2, 79.4, 173.3 ppm; SEC: R_t=33.66 min; HRMS (ESI) calcd for $C_{37}H_{66}N_2O_2+H^+$: 571.5202; found: 571.5239; elemental analysis calcd (%) for $C_{37}H_{66}N_2O_2$: C 77.84, H 11.65, N 4.90; found: C 78.06, H 12.22, N 4.91.

G3-Diacetylene 5-G3: DCC (0.05 g, 0.24 mmol) was added to a stirred solution of **9-G3** (0.18 g, 0.17 mmol), propargylamine (0.1 mL, 1.56 mmol), HOBt (0.04 g, 0.30 mmol), and DMAP (2 mg) in CH$_2$Cl$_2$ (15 mL). The reaction mixture was stirred at 25 °C for 2 h and concentrated under reduced pressure. The residue was purified by flash chromatography on silica gel (eluent: hexane/EtOAc 18:1) to afford **5-G3** (0.16 g, 88%) as a colorless oil. R_f=0.17 (hexane/EtOAc 18:1). ^{1}H NMR (400 MHz, CDCl$_3$): δ=0.87 (d, J=6.4 Hz, 48H; CH$_3$), 1.05–1.30 (m, 70H), 1.47 (septet, J=6.4 Hz, 8H; C*H*Me$_2$), 1.75–1.85 (m, 4H; CCH$_2$), 2.19 (t, J=2.4 Hz, 2H; C≡CH), 4.06 (dd, J=5.2, 2.4 Hz, 2H; CH$_2$C≡C), 7.40 ppm (t, J=5.2 Hz, 2H; NH); ^{13}C NMR (100 MHz, CDCl$_3$): δ=22.2, 22.80, 22.82, 23.7, 28.4, 29.2, 31.25, 31.30, 33.9, 34.2, 34.3, 35.9, 36.0, 37.3, 37.8, 38.8, 56.9, 71.3, 79.5, 173.2 ppm; SEC: R_t=31.87 min. MS (ESI): m/z (%): 1098 (100) [M+Na$^+$]; HRMS (ESI) calcd for $C_{73}H_{138}N_2O_2+Na^+$: 1098.0651; found: 1098.0634; elemental analysis calcd (%) for $C_{73}H_{138}N_2O_2$: C 81.49, H 12.93, N 2.60; found: C 81.72, H 13.00, N 2.78.

Polymer 2-G1G1: Sodium ascorbate (30 mg, 0.15 mmol) and CuSO$_4$·5H$_2$O (8 mg, 0.03 mmol) were added to a solution of **4-G1** (164 mg, 0.31 mmol) and **5-G1** (98 mg, 0.31 mmol) in THF/DMF/H$_2$O (v/v/v 1:1:1, 6 mL). The mixture was stirred at 25 °C for 4 d. Aqueous HCl (25 mL, 0.2 M) was added to the solution and the precipitate was filtered off to give the polymer as a yellow solid (240 mg, 92%). ^{1}H NMR (400 MHz, [D$_6$]DMSO): δ=0.50–1.00 (m, 32H; CH$_2$, CH$_3$), 1.11–1.50 (m, 4H; C*H*Me$_2$), 1.60–2.00 (m, 8H; CCH$_2$), 4.00–4.60 (m, 8H; TriazC*H$_2$*Ar, NHC*H$_2$*Ar), 5.30–5.70 (m, 4H; NHC*H$_2$*Triaz), 7.00–7.40 (m, 8H; Ar*H*), 7.80–8.10 (m, 2H; Triaz*H*), 8.60–9.10 ppm (m, 4H; NH); ^{13}C NMR (100 MHz, [D$_6$]DMSO): δ=22.2, 27.5, 27.7, 32.9, 33.0, 34.3, 41.9, 52.4, 56.0, 123.1, 127.2, 127.4, 127.7, 128.1, 133.8, 134.2, 139.4, 139.6, 172.7 ppm.

Polymer 2-G1G2: Sodium ascorbate (55 mg, 0.28 mmol) and CuSO$_4$·5H$_2$O (14 mg, 0.06 mmol) were added to a solution of **4-G1** (295 mg, 0.55 mmol) and **5-G2** (316 mg, 0.55 mmol) in THF/DMF/H$_2$O (v/v/v 1:1:1, 6 mL). The reaction mixture was stirred at 25 °C for 4 d. Aqueous HCl (25 mL, 0.2 M) was added to the solution and the precipitate was filtered off to give the polymer as a yellow solid (595 mg, 97%). ^{1}H NMR (400 MHz, [D$_8$]THF): δ=0.60–0.94 (m, 36H; CH$_3$), 0.94–1.30 (m, 30H), 1.31–1.58 (m, 6H; C*H*Me$_2$), 1.76–2.00 (m, 8H; CCH$_2$), 4.00–4.50 (m, 8H; TriazC*H$_2$*Ar, NHC*H$_2$*Ar), 5.30–5.60 (m, 4H; NHC*H$_2$*Triaz), 6.95–7.42 (m, 8H; Ar*H*), 7.50–7.80 (m, 2H; Triaz*H*), 7.88–8.30 (m, 2H; NH), 8.40–8.65 ppm (m, 2H; NH); ^{13}C NMR (100 MHz, [D$_8$]THF): δ=22.6, 23.2, 23.4, 26.5, 29.5, 32.1, 34.8, 35.1, 36.0, 36.8, 38.6, 43.6, 54.1, 57.6, 58.0, 123.4, 129.0, 135.7, 141.0, 146.6, 173.6, 174.2 ppm.

Polymer 2-G1G3: Sodium ascorbate (29 mg, 0.15 mmol) and CuSO$_4$·5H$_2$O (7 mg, 0.03 mmol) were added to a solution of **4-G1** (154 mg, 0.29 mmol) and **5-G3** (311 mg, 0.29 mmol) in THF/DMF/H$_2$O (v/v/v 1:1:1, 6 mL). The reaction mixture was stirred at 25 °C for 4 d. Aqueous HCl (25 mL, 0.2 M) was added to the solution and the precipitate was filtered off to give the polymer as a yellow solid (425 mg, 91%). ^{1}H NMR (400 MHz, [D$_8$]THF): δ=0.70–0.95 (m, 60H; CH$_3$), 0.96–1.07 (m, 4H; CH$_2$), 1.08–1.37 (m, 70H), 1.41–1.61 (m, 10H; C*H*Me$_2$), 1.75–1.95 (m, 8H; CCH$_2$), 4.20–4.50 (m, 8H; TriazC*H$_2$*Ar, NHC*H$_2$*Ar), 5.30–5.60 (m, 4H; NHC*H$_2$*Triaz), 7.10–7.30 (m, 8H; Ar*H*), 7.60–7.82 (m, 2H; Triaz*H*), 7.84–7.97 (m, 1H; NH), 8.00–8.15 (m, 1H; NH), 8.45–8.60 ppm (m, 2H; NH); ^{13}C NMR (100 MHz, [D$_8$]THF): δ=22.6, 23.2, 23.4, 24.7, 29.5, 29.7, 30.8, 32.3, 32.4, 34.5, 35.0, 35.3, 35.5, 35.9, 37.0, 38.2, 39.1, 43.6, 54.0, 54.1, 57.6, 57.8, 58.0, 58.1, 123.3, 128.8, 128.9, 129.0, 130.4, 135.7, 135.8, 141.1, 146.7, 173.5, 173.6, 174.2 ppm.

Polymer 2-G2G1: Sodium ascorbate (52 mg, 0.26 mmol) and CuSO$_4$·5H$_2$O (13 mg, 0.05 mmol) were added to a solution of **4-G2** (409 mg, 0.52 mmol) and **5-G1**(166 mg, 0.52 mmol) in THF/DMF/H$_2$O (v/v/v 1:1:1, 6 mL). The reaction mixture was stirred at 25 °C for 4 d. Aqueous HCl (25 mL, 0.2 M) was added to the solution and the precipitate was filtered off to give the polymer as a yellow solid (567 mg, 99%). ^{1}H NMR (400 MHz, [D$_8$]THF): δ=0.50–0.75 (m, 14H), 0.75–1.00 (m, 30H), 1.00–1.37 (m, 22H), 1.38–1.59 (m, 6H; C*H*Me$_2$), 1.77–2.10 (m, 8H; CCH$_2$), 3.83–4.50 (m, 8H; TriazC*H$_2$*Ar, NHC*H$_2$*Ar), 5.20–5.60 (m, 4H; NHC*H$_2$*Triaz), 7.00–7.30 (m, 8H; Ar*H*), 7.52–7.94 (m, 2H; Triaz*H*), 8.00–8.70 ppm (m, 4H; NH); ^{13}C NMR (100 MHz, [D$_8$]THF): δ=23.1, 23.4, 29.3, 29.5, 32.2, 34.5, 35.1, 35.6, 36.9, 38.7, 43.7, 54.1, 57.6, 58.0, 123.7, 128.7, 129.1, 135.6, 141.0, 146.6, 174.0 ppm.

Polymer 2-G2G2: Sodium ascorbate (40 mg, 0.20 mmol) and CuSO$_4$·5H$_2$O (10 mg, 0.04 mmol) were added to a solution of **4-G2** (325 mg, 0.41 mmol) and **5-G2** (236 mg, 0.41 mmol) in THF/DMF/H$_2$O (v/v/v 1:1:1, 6 mL). The reaction mixture was stirred at 25 °C for 4 d. Aqueous HCl (25 mL, 0.2 M) was added to the solution and the precipitate was filtered off to give the polymer as a yellow solid (527 mg, 94%). ^{1}H NMR (400 MHz, [D$_8$]THF): δ=0.70–1.00 (m, 48H; CH$_3$), 1.01–1.38 (m, 52H), 1.39–1.63 (m, 8H; C*H*Me$_2$), 1.75–2.16 (m, 8H; CCH$_2$), 4.00–4.50 (m, 8H; TriazC*H$_2$*Ar, NHC*H$_2$*Ar), 5.35–5.65 (m, 4H; NHC*H$_2$*Triaz), 7.00–7.30 (m, 8H; Ar*H*), 7.50–7.78 (m, 2H; Triaz*H*), 7.79–7.90 (m, 2H; NH), 8.10–8.25 (m, 1H; NH), 8.25–8.40 ppm (m, 1H; NH); ^{13}C NMR (100 MHz, [D$_8$]THF): δ=22.3, 22.4, 22.6, 23.0, 23.4, 29.5, 32.2, 34.4, 34.6, 35.2, 36.0, 36.3, 36.9, 38.56, 38.64, 43.7, 53.9, 54.1, 57.9, 58.2, 123.3, 128.6, 128.8, 129.0, 135.7, 135.9, 140.9, 146.6, 173.3, 173.7, 174.0 ppm.

Polymer 2-G2G3: Sodium ascorbate (14 mg, 0.07 mmol) and CuSO$_4$·5H$_2$O (3 mg, 0.01 mmol) were added to a solution of **4-G2** (108 mg, 0.14 mmol) and **5-G3** (148 mg, 0.14 mmol) in THF/DMF/H$_2$O (v/v/v 1:1:1, 6 mL). The reaction mixture was stirred at 25 °C for 4 d and then extracted with CH$_2$Cl$_2$ (3×20 mL). The combined extracts were washed with brine, dried (Mg$_2$SO$_4$), filtered, and evaporated in vacuo to give the polymer as a pale yellow solid (223 mg, 87%). ^{1}H NMR (400 MHz, [D$_8$]THF): δ=0.85–0.95 (m, 72H; CH$_3$), 1.10–1.39 (m, 96H), 1.41–1.57 (m, 12H; C*H*Me$_2$), 1.74–1.95 (m, 8H; CCH$_2$), 4.25–4.45 (m, 8H; TriazC*H$_2$*Ar, NHC*H$_2$*Ar), 5.40–5.60 (m, 4H; NHC*H$_2$*Triaz), 7.05–7.28 (m, 8H; Ar*H*), 7.56–7.60 and 7.80–7.83 (m, 2H; Triaz*H*), 7.70–7.80 (m, 1H; NH), 8.00–8.10 (m, 1H; NH), 8.40–8.50 ppm (m, 2H; NH); ^{13}C NMR (100 MHz, [D$_8$]THF): δ=22.4, 23.1, 23.4, 24.7, 29.5, 30.8, 32.2, 32.3, 32.4, 34.4, 34.6, 34.9, 35.1, 35.2, 35.3, 35.49, 35.54, 36.0, 36.3, 36.9, 37.0, 38.0, 38.2, 38.6, 38.7, 39.0, 43.7, 53.9, 54.1, 57.9, 58.20, 58.24, 123.2, 123.3, 128.6, 128.7, 128.8, 129.0, 135.8, 135.9, 140.9, 141.0, 146.5, 146.6, 173.3, 173.4, 173.6, 174.1 ppm.

Polymer 2-G3G1: Sodium ascorbate (37 mg, 0.19 mmol) and CuSO$_4$·5H$_2$O (11 mg, 0.04 mmol) were added to a solution of **4-G3** (485 mg, 0.38 mmol) and **5-G1** (120 mg, 0.38 mmol) in THF/DMF/H$_2$O (v/v/v 1:1:1, 6 mL). The reaction mixture was stirred at 25 °C for 4 d. Aqueous HCl (25 mL, 0.2 M) was added to the solution and the precipitate was filtered off to give the polymer as a yellow solid (542 mg, 92%). ^{1}H NMR (400 MHz, [D$_8$]THF): δ=0.68–0.79 (m, 48H; CH$_3$), 0.80–1.00 (m, 12H), 1.07–1.42 (m, 74H), 1.43–1.63 (m, 10H; C*H*Me$_2$), 1.75–2.11 (m, 8H; CCH$_2$), 4.20–4.45 (m, 8H; TriazC*H$_2$*Ar, NHC*H$_2$*Ar), 5.40–5.55 (m, 4H; NHC*H$_2$*Triaz), 7.08–7.28 (m, 8H; Ar*H*), 7.60–7.80 (m, 2H; Triaz*H*), 7.90–8.00 (m, 1H; NH), 8.10–8.20 (m, 2H; NH), 8.35–8.55 ppm (m, 1H; NH); ^{13}C NMR (100 MHz, [D$_8$]THF): δ=23.1, 23.4, 24.7, 29.35, 29.44, 29.5, 29.7, 30.8, 32.3, 32.4, 34.5, 34.6, 35.0, 35.3, 35.5, 35.8, 37.0, 38.16, 38.22, 39.0, 43.7, 53.9, 54.1, 57.4, 57.7, 58.0, 58.1, 123.4, 128.5, 128.8, 128.9, 129.0, 129.2, 135.7, 135.8, 140.9, 141.0, 146.6, 173.4, 173.6, 173.8, 174.1 ppm.

Polymer 2-G3G2: Sodium ascorbate (30 mg, 0.15 mmol) and CuSO$_4$·5H$_2$O (8 mg, 0.03 mmol) were added to a solution of **4-G3** (395 mg, 0.31 mmol) and **5-G2** (175 mg, 0.31 mmol) in THF/DMF/H$_2$O (v/v/v 1:1:1, 6 mL). The reaction mixture was stirred at 25 °C for 4 d and then extracted with CH$_2$Cl$_2$ (3×20 mL). The combined extracts were washed with brine, dried (Mg$_2$SO$_4$), filtered and evaporated in vacuo to give the polymer as a pale yellow solid (526 mg, 92%). ^{1}H NMR (400 MHz, [D$_8$]THF): δ=0.80–0.99 (m, 72H; CH$_3$), 1.00–1.41 (m, 96H), 1.42–1.62 (m, 12H; C*H*Me$_2$), 1.75–2.02 (m, 8H; CCH$_2$), 4.10–4.50 (m, 8H; TriazC*H$_2$*Ar and NHC*H$_2$*Ar), 5.35–5.70 (m, 4H; NHC*H$_2$*Triaz), 7.00–7.25 (m, 8H; Ar*H*), 7.55–7.71 (m, 2H; Triaz*H*), 7.72–7.90 (m, 2H; NH), 8.10–8.30 ppm (m, 2H; NH); ^{13}C NMR (100 MHz, [D$_8$]THF): δ=22.2, 22.4, 22.5, 22.9, 23.4, 24.7, 29.5, 32.1, 32.2, 32.3, 35.0, 35.2, 35.3, 35.4, 35.5, 36.8, 37.0, 38.2, 38.50, 38.54, 39.0, 43.8, 53.9, 54.1, 57.9, 58.0, 58.3, 123.3, 128.6, 128.8, 129.0, 129.6, 135.5, 135.6, 135.8, 140.8, 141.0, 146.5, 173.2, 173.3, 173.6, 173.76, 173.84 ppm.

Polymer 2-G3G3: Sodium ascorbate (10 mg, 0.05 mmol) and $CuSO_4 \cdot 5H_2O$ (3 mg, 0.01 mmol) were added to a solution of **4-G3** (126 mg, 0.10 mmol) and **5-G3** (106 mg, 0.10 mmol) in THF/DMF/H_2O (v/v/v 1:1:1, 6 mL). The reaction mixture was stirred at 25 °C for 8 d and then extracted with CH_2Cl_2 (3×20 mL). The combined extracts were washed with brine, dried (Mg_2SO_4), filtered and evaporated in vacuo to give the polymer as a pale yellow solid (196 mg, 84 %). ^{1}H NMR (400 MHz, [D$_8$]THF): $\delta = 0.89$ (d, $J = 6.8$ Hz, 96 H; CH_3), 1.10–1.40 (m, 140 H), 1.50 (septet, $J = 6.8$ Hz, 16 H; C*H*Me$_2$), 1.76–1.99 (m, 8 H; CCH_2), 4.25–4.45 (m, 8 H; TriazC*H*$_2$Ar, NHC*H*$_2$Ar), 5.40–5.60 (m, 4 H; NHC*H*$_2$Triaz), 7.05–7.30 (m, 8 H; Ar*H*), 7.55–7.71 (m, 2 H; Triaz*H*), 7.80–7.90 (m, 2 H; NH), 8.10–8.20 (m, 1 H; NH), 8.30–8.48 ppm (m, 1 H; NH); ^{13}C NMR (100 MHz, [D$_8$]THF): $\delta = 22.5$, 23.4, 24.7, 29.6, 32.36, 32.39, 35.0, 35.3, 35.6, 37.1, 38.2, 39.1, 43.8, 53.9, 54.1, 58.0, 58.25, 58.30, 123.1, 123.4, 128.6, 128.7, 128.9, 129.0, 129.2, 135.8, 135.9, 141.0, 141.1, 146.6, 173.1, 173.2, 173.7, 174.0 ppm.

Acknowledgements

We thank the Research Grants Council, Hong Kong SAR, for financial support (Project No: 400810).

---

[1] a) C. W. Tornøe, C. Christensen, M. Meldal, *J. Org. Chem.* **2002**, *67*, 3057; b) V. V. Rostovtsev, L. G. Green, V. V. Fokin, K. B. Sharpless, *Angew. Chem.* **2002**, *114*, 2708; *Angew. Chem. Int. Ed.* **2002**, *41*, 2596.

[2] For examples, see a) B. C. Englert, S. Bakbak, U. H. F. Bunz, *Macromolecules* **2005**, *38*, 5868; b) S. Bakbak, P. J. Leech, B. E. Carson, S. Saxena, W. P. King, U. H. F. Bunz, *Macromolecules* **2006**, *39*, 6793; c) A. Qin, C. K. W. Jim, W. Lu, J. W. Y. Lam, M. Häussler, Y. Dong, H. H. Y. Sung, I. D. Williams, G. K. L. Wong, B. Z. Tang, *Macromolecules* **2007**, *40*, 2308; d) A. Qin, J. W. Y. Lam, C. K. W. Jim, L. Zhang, J. Yan, M. Häussler, J. Liu, Y. Dong, D. Liang, E. Chen, G. Jia, B. Z. Tang, *Macromolecules* **2008**, *41*, 3808; e) B. Z. Tang, *Macromol. Chem. Phys.* **2008**, *209*, 1303.

[3] For reviews on click polymerizations, see a) W. H. Binder, C. Kluger, *Curr. Org. Chem.* **2006**, *10*, 1791; b) V. D. Bock, H. Hiemstra, J. H. van Maarseveen, *Eur. J. Org. Chem.* **2006**, 51; c) P. Wu, V. V. Fokin, *Aldrichimica Acta* **2007**, *40*, 7; d) W. H. Binder, R. Sachsenhofer, *Macromol. Rapid Commun.* **2007**, *28*, 15; <*lit* e>M. V. Gil, M. J. Arévalo, O. López, *Synthesis* **2007**, 1589; f) J. E. Moses, A. D. Moorhouse, *Chem. Soc. Rev.* **2007**, *36*, 1249; g) J.-F. Lutz, *Angew. Chem.* **2007**, *119*, 1036; *Angew. Chem. Int. Ed.* **2007**, *46*, 1018; h) M. Meldal, C. W. Tornøe, *Chem. Rev.* **2008**, *108*, 2952.

[4] H.-F. Chow, K.-N. Lau, Z. Ke, Y. Liang, C.-M. Lo, *Chem. Commun.* **2010**, *46*, 3437.

[5] a) Y. Li, A. H. Flood, *Angew. Chem.* **2008**, *120*, 2689; *Angew. Chem. Int. Ed.* **2008**, *47*, 2649; b) H. Juwarker, J. M. Lenhardt, D. M. Pham, S. L. Craig, *Angew. Chem.* **2008**, *120*, 3800; *Angew. Chem. Int. Ed.* **2008**, *47*, 3740.

[6] H. Isobe, T. Fujino, N. Yamazaki, M. Guillot-Nieckowski, E. Nakamura, *Org. Lett.* **2008**, *10*, 3729.

[7] X.-M. Liu, A. Thakur, D. Wang, *Biomacromolecules* **2007**, *8*, 2653.

[8] D. D. Díaz, K. Rajagopal, E. Strable, J. Schneider, M. G. Finn, *J. Am. Chem. Soc.* **2006**, *128*, 6056.

[9] K.-N. Lau, H.-F. Chow, M.-C. Chan, K.-W. Wong, *Angew. Chem.* **2008**, *120*, 7018; *Angew. Chem. Int. Ed.* **2008**, *47*, 6912.

[10] For examples of dendrons and dendrimers with gelating properties, see a) G. R. Newkome, G. R. Baker, S. Arai, M. J. Saunders, P. S. Russo, K. J. Theriot, C. N. Moorefield, L. E. Rogers, J. E. Miller, T. R. Lieux, M. E. Murray, B. Phillips, L. Pascal, *J. Am. Chem. Soc.* **1990**, *112*, 8458; b) W.-D. Jang, D.-L. Jiang, T. Aida, *J. Am. Chem. Soc.* **2000**, *122*, 3232; c) C. Kim, K. T. Kim, Y. Chang, H. H. Song, T.-Y. Cho, H.-J. Jeon, *J. Am. Chem. Soc.* **2001**, *123*, 5586; d) K. S. Partridge, D. K. Smith, G. M. Dykes, P. T. McGrail, *Chem. Commun.* **2001**, 319; e) H.-F. Chow, J. Zhang, *Chem. Eur. J.* **2005**, *11*, 5817; f) H.-F. Chow, J. Zhang, *Tetrahedron* **2005**, *61*, 11279; g) Y. Ji, Y.-F. Luo, X.-R. Jia, E.-Q. Chen, Y. Huang, C. Ye, B.-B. Wang, Q.-F. Zhou, Y. Wei, *Angew. Chem.* **2005**, *117*, 6179; *Angew. Chem. Int. Ed.* **2005**, *44*, 6025; h) W.-S. Li, X.-R. Jia, B.-B. Wang, Y. Ji, Y. Wei, *Tetrahedron* **2007**, *63*, 8794; i) D. Astruc, E. Boisselier, C. Ornelas, *Chem. Rev.* **2010**, *110*, 1857.

[11] H.-F. Chow, K.-F. Ng, Z.-Y. Wang, C.-H. Wong, T. Luk, C.-M. Lo, Y.-Y. Yang, *Org. Lett.* **2006**, *8*, 471.

[12] M. M. Schiavoni, H.-G. Mack, S. E. Ulic, C. O. Della Védova, *Spectrochim. Acta Part A* **2000**, *56*, 1533.

[13] A.-D. Schlüter, *Top. Curr. Chem.* **2005**, *245*, 151.

Received: April 6, 2011